nutrients

MDPI

Article

Botanical Mixture Containing Nitric Oxide Metabolite Enhances Neural Plasticity to Improve Cognitive Impairment in a Vascular Dementia Rat Model

Xiaorong Zhang [1,2,3,†], Seung-Bum Yang [4,†], Lin Cheng [5], Koo Ho [3] and Min-Sun Kim [3,*]

[1] Department of Pathology, Affiliated Hospital of Jiujiang University, Jiujiang 332000, China
[2] Center for Cognitive Science and Transdisciplinary Studies, Jiujiang University, Jiujiang 332000, China
[3] Center for Nitric Oxide Metabolite, Wonkwang University, Iksan 54538, Republic of Korea
[4] Department of Medical Non-Commissioned Officer, Wonkwang Health Science University, Iksan 54538, Republic of Korea
[5] Jiujiang Clinical Precision Medicine Research Center, Jiujiang 332000, China
* Correspondence: mskim@wku.ac.kr; Tel.: +82-63-850-6779
† These authors contributed equally to this work.

Abstract: Vascular dementia (VD), caused by impaired cerebral blood flow, is the most common form of dementia after Alzheimer's disease (AD) in the elderly and is characterized by severe neuronal damage and cognitive decline. Nitric oxide (NO) is an important determinant of vascular homeostasis, and its deficiency is associated with the progression of VD. In this study, we investigated the role of nitrite ion, a NO metabolite in a botanical mixture (BM) of fermented garlic, fermented *Scutellaria baicalensis*, and *Rhodiola rosea* on neuron loss and cognitive impairment using a VD rat model. The BM containing the NO metabolite alleviated cognitive deficits and enhanced neural plasticity, as reflected by an increase in long-term potentiation. The BM also alleviated neuron apoptosis, decreased GFAP expression, and oxidative stress, and increased parvalbumin and brain-derived neurotrophic factor (BDNF) levels. These results indicate that BM exerts neuroprotective effects and alleviates cognitive dysfunction while enhancing neuroplasticity, and thus has therapeutic potential against VD.

Keywords: vascular dementia; long-term potentiation; parvalbumin; nitric oxide; *Scutellaria baicalensis*; *Rhodiola rosea*

check for updates

Citation: Zhang, X.; Yang, S.-B.; Cheng, L.; Ho, K.; Kim, M.-S. Botanical Mixture Containing Nitric Oxide Metabolite Enhances Neural Plasticity to Improve Cognitive Impairment in a Vascular Dementia Rat Model. *Nutrients* **2023**, *15*, 4381. https://doi.org/10.3390/nu15204381

Academic Editor: Panteleimon Giannakopoulos

Received: 12 August 2023
Revised: 12 September 2023
Accepted: 9 October 2023
Published: 16 October 2023

Copyright: © 2023 by the authors. Licensee MDPI, Basel, Switzerland. This article is an open access article distributed under the terms and conditions of the Creative Commons Attribution (CC BY) license (https://creativecommons.org/licenses/by/4.0/).

1. Introduction

Vascular dementia (VD) is the second most common form of dementia after Alzheimer's disease (AD); it is caused by impaired cerebral blood flow. VD is characterized by severe neuronal damage, cognitive decline, white matter lesions, neurodegeneration, synapse and dendritic spine loss, and neuroinflammation, and can eventually lead to death [1,2]. There are currently no effective therapies for VD and treatments are mainly symptomatic. The prevalence of VD is increasing worldwide with the aging of the population, and there is, therefore, an urgent need for new treatment approaches.

Nitric oxide (NO) is a key signaling molecule in cell–cell communication; it is produced in cells by NO synthase (NOS) [3] and plays an important role in various biological processes in the central nervous system, including the modulation of cerebral blood flow, synaptic plasticity, neuroinflammation, oxidative stress, and apoptosis [4]. NO depletion plays an important role in VD pathogenesis [5]; thus, therapeutic strategies that increase NO levels may be beneficial in VD. Recent studies showed that various reductase can reduce the nitrite ion to NO, increasing NO bioavailability in the body. Thus, nitrite is considered as a NO metabolite [6,7].

Garlic is a plant that has medicinal value owing to its demonstrated capacity to modulate immune function [8] and reduce cardiovascular disease risk [9], and for its antidiabetic and antihypertensive properties [10]. Our previous study has demonstrated that fermented

garlic, enriched in NO metabolites, increased systemic blood flow by activating intracellular nitric oxide signaling [11]. *Scutellaria baicalensis* is a flowering plant that has been widely used to treat of various neurodegenerative diseases. *S. baicalensis* and its extract have cytoprotective and anti-inflammatory effects related to the reduction in reactive oxygen species (ROS) accumulation and alleviation of mitochondrial damage [12,13]. *Rhodiola rosea*, another flowering plant, has been widely used to stimulate the nervous system and can attenuate anxiety, enhance work performance and the capacity for physical work, and improve memory and learning in rat models [14,15]. Additionally, *S. baicalensis* and *R. rosea* can increase NO production and bioavailability [16,17].

To determine whether the NO metabolite that increases NO bioavailability can be used to prevent or treat VD, the present study investigated the effects of a mixture of fermented garlic extract, fermented *S. baicalensis*, and *R. rosea* on neural plasticity and memory function in a VD rat model.

2. Materials and Methods

2.1. Animals

Adult male Sprague Dawley rats (three groups of 12 rats each, and the experiment was repeated three times) aged 7–8 weeks (Samtako Bio, Seoul, Republic of Korea), weighing 200–250 g on arrival, were housed in groups of three per cage under controlled laboratory conditions (12:12 h light/dark cycle, lights on at 7:00 a.m., 22 ± 2 °C, 45–55% humidity). The rats had ad libitum access to food and water. All experiments were approved by the Laboratory Animal Ethics Committee of Wonkwang University (WKU20-12, approval date: 23 January 2020).

2.2. BCCAO Surgery

Permanent bilateral occlusion of the common carotid arteries (BCCAO) in rats is used to investigate the cognitive decline and neurodegenerative processes associated with VD [18,19]. The animals were randomly divided into three groups (n = 12 per group): (1) sham-operated, (2) BCCAO, and (3) BCCAO + treatment with the botanical mixture (BM) containing NO metabolite (4 mL/kg administered twice a day for 4 weeks). The rats were anesthetized with an intraperitoneal injection of ketamine (5 mg/kg) and BCCAO was performed as previously described [20]. Briefly, an incision was made in the middle of the neck; the two sides of the common carotid artery and vagus nerve were carefully separated, and the common carotid artery was then permanently ligated with a silk suture (4-0). Sham-operated rats underwent the same procedure but without common carotid artery ligation.

2.3. BM Preparation and Administration

BM consisted of NO metabolite (2000 ppm of nitrite in 1.5 mL of diluted fermented garlic extract), ethanol extract of fermented *S. baicalensis* (1 g), and fermented *R. rosea* (1 g), both diluted in 50 mL of distilled water. The fermented garlic extract was supplied by HumanEnos (Wanju-gun, Jeonbuk, Republic of Korea). Rats in the BCCAO+BM group started receiving BM treatment on day 2 after the BCCAO surgery. The treatment lasted 4 weeks (4 mL/kg twice a day, oral administration) (10:00 a.m. and 4:00 p.m.). The rats in the sham and BCCAO groups received the same volume of saline (vehicle).

2.4. Y-Maze Test

Four weeks after BCCAO surgery, the Y-maze was performed to assess spatial learning and memory (Figure 1A) [20]. All animals were trained daily at 3:00 p.m. Training times and conditions were consistent, and all the training was carried out by the same researcher. The Y-maze consisted of three arms (A, B, and C) evenly spaced at a 120° angle. The animals were placed in the center of the Y-maze and allowed to freely explore for 8 min. The sequence of entries into each arm by each rat was recorded by a video tracking and analysis system.

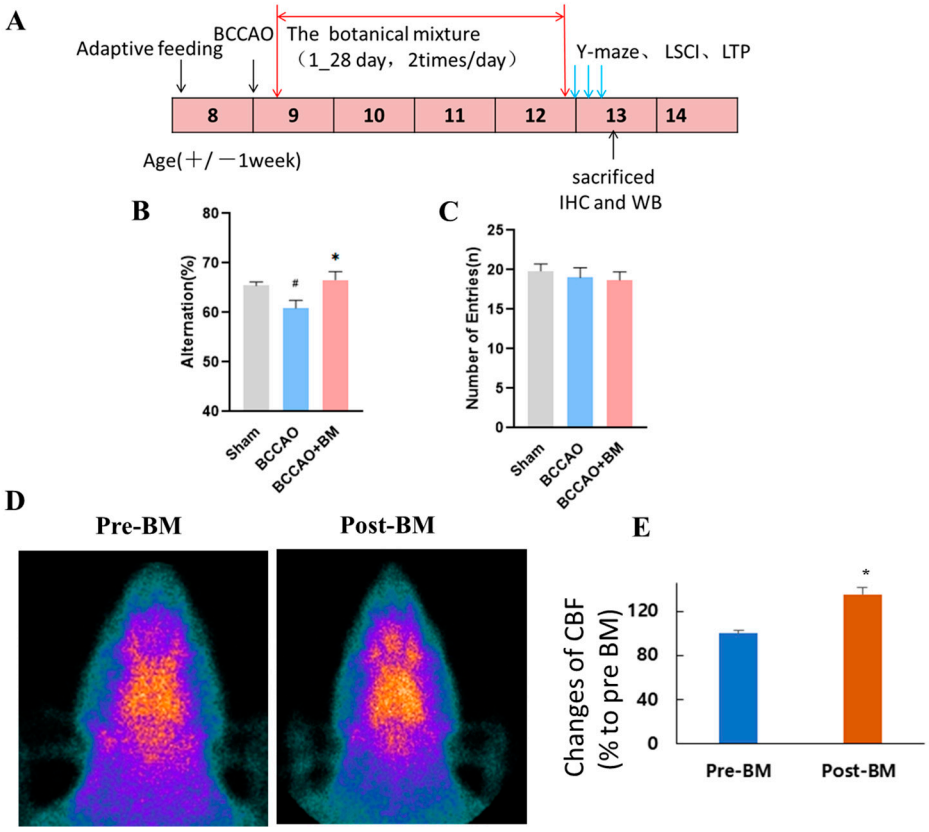

Figure 1. Botanical mixture alleviates cognitive deficits in a rat model of VD. (**A**) Treatment schedule for establishing the BCCAO rat model. (**B**) Performance in the Y-maze test at 4 weeks after BCCAO. (**C**) Number of arm entries in the Y-maze test. (**D**) Change in cerebral blood flow evaluated by SPECT imaging using 99mTcHMPAO tracer (n = 3). (**E**) Bar histogram showing changes in the cerebral blood flow (CBF) calculated by cerebral hemisphere/neck soft tissue uptake ratios before and after treatment of BM in 3 BACCO rats. Values represent percent ratio of CBF of Post-BM to that of Pre-BM and are mean ± SD (n = 3, * $p < 0.05$ Pre-BM vs. Post-BM). # $p < 0.05$ vs. sham; * $p < 0.05$ vs. BCCAO (Y-maze, n = 12 per group).

2.5. Brain-Perfusion SPECT Imaging

Tc-99m ECD (~185 MBq) was injected intravenously into the rats. After 30 min, brain images were acquired using a gamma camera equipped with a 3 mm pinhole collimator (Vertex; ADAC Laboratories, Milpitas, CA, USA) with the following settings: window setting at 140 keV, width of 20%, and acquisition time of 150 s. The images were saved in a 512 × 512 matrix. Regions of interest were manually drawn in the cerebral hemisphere, brain stem, and neck soft tissue areas for analysis. The cerebral hemisphere/brain stem (Cb/bs) and cerebral hemisphere/neck soft tissue (Cb/neck) uptake ratios were calculated using the mean radioactivity of the brain stem and neck soft tissue as a reference.

Brain perfusion images were obtained from three animals four weeks after BCCAO. Following general anesthesia using 3% isoflurane, a baseline brain perfusion image was acquired. Three days later, the rats with BCCAO were re-anesthetized and orally administered a 1 mL injection of BM mixture. After the treatment, brain perfusion images were obtained using the same method as described above. The percentage differences of Cb/bs and Cb/neck before and after treatment were calculated.

2.6. Long-Term Potentiation (LTP) in the Hippocampus

Animals were anesthetized with urethane (12 mg/kg) and their head was fixed on a stereotaxis system. The skull and dura were removed, and a bipolar metal stimulation electrode was inserted into the CA3 area of the hippocampus (anterior–posterior [AP],

4.0 mm; dorsal–ventral [DV], 3.5 mm; medial–lateral [ML], 3.5 mm from bregma). A tungsten recording electrode was used to record field-evoked excitatory postsynaptic potentials (fEPSPs) in the CA1 area (AP, −3.0 mm; ML, 1.5–2.5 mm; DV, 2.6 mm). The change in fEPSP amplitude as stimulus intensity gradually increased from 0.01 to 0.2 mA was recorded, and the stimulus intensity eliciting the maximum fEPSP amplitude and 50% of the maximum amplitude was determined.

To induce LTP, electric stimulation was delivered in a theta-burst stimulation (TBS) pattern in the CA3 region three times at 1 min intervals. TBS consisted of a repetitive burst waveform (five pulses, 100 Hz) composed of five square waves at 10-ms intervals, delivered five times at 200-ms intervals (5 Hz). After TBS, fEPSPs were induced and recorded for 60 min in the same manner. After the recording, a 0.3-mA positive current was delivered via the recording electrode for 20 s to create a lesion in the CA1 and CA3 regions of the hippocampus. The location of the stimulation and recording electrodes was confirmed by Cresyl Violet staining. Signal 2.0 (Cambridge Electronic Design, Cambridge, UK) and Excel 2013 (Microsoft, Redmond, WA, USA) software programs were used to analyze fEPSP signals.

2.7. Immunohistochemistry

Rats were anesthetized with urethane (12 mg/kg), then transcardially perfused with 1% paraformaldehyde (PFA) and 4% PFA dissolved in a 0.2 M phosphate buffer and decapitated. The brain was removed carefully and quickly fixed in 4% PFA overnight at 4 °C, and immersed in a 30% sucrose solution for 3 days at 4 °C. Coronal brain sections (35-µm thick) were cut using a freezing microtome and incubated for 4 min at 95 °C with an antigen retrieval solution. After being washed with phosphate-buffered saline (PBS), the sections were rinsed with 0.5% PBS and 0.1% Triton X-100 containing 3% goat serum, followed by overnight incubation at 4 °C with primary antibodies against nitrotyrosine (Millipore, Billerica, MA, USA; cat. no. 06-284, 1:300), parvalbumin (PV) (Abcam, Cambridge, MA, USA; cat. no. ab11427, 1:2000), and neuronal nuclei (NeuN) (Abcam; cat. no. ab128886, 1:1000). They were then washed with 0.05% PBS and incubation for 1 h with horseradish peroxidase (HRP)-conjugated anti-rabbit IgG (Golden Bridge International Labs, Uden, The Netherlands; cat. no. D13-110). Immunoreactivity was visualized with 0.05% diaminobenzidine (DAB) in hydrochloric acid and 0.003% H_2O_2. The tissue was washed with 0.1 M phosphate buffer, mounted on gel-coated slides, dehydrated, cleared with xylene, and mounted on slides; microscopy pictures were then recorded. Three sections per brain and three fields per section were used for quantification and the ImageJ software (1.8.0) was used to calculate the total number or strength of positive cells in each field.

2.8. Cresyl Violet Staining

The rat brain sections were rinsed for 2 min with 100% alcohol and xylene for 2 min, followed by 100%, 70%, and 20% alcohol for 2 min each. The sections were then incubated in a 0.1% Cresyl Violet solution for 5 min, then washed with distilled water, differentiated in 95% alcohol for 1 min, dehydrated in 100% alcohol for 2 min, cleared in xylene, and mounted using a DPX mounting medium.

2.9. Western Blot Analysis

Cortex and hippocampus tissues were homogenized in a buffer containing 1× inhibitor cocktail and 0.5 mM EDTA solution. Total proteins were quantified with a BCA Protein Assay Kit, and a sample of proteins (20 µg) was separated on a 10%, 12%, or 15% sodium dodecyl sulfate (SDS)-polyacrylamide gel for 90 min at 100 V and transferred to an Immobilon P membrane that was blocked with 5% dried milk protein for 1 h, rinsed three times with 0.05% Tween-20 (TBST), and incubated with primary antibodies against PV, BDNF (Abcam; cat. no. ab108319), β-actin (Calbiochem, San Diego, CA, USA; cat. no. D00024369), and glial fibrillary acidic protein (GFAP) (Abcam; cat. no. ab7260) overnight at 4 °C. The membrane was washed three times with TBST for 10 min and incubated

with HRP-conjugated secondary antibody anti-rabbit (1:5000, Santa Cruz Biotechnology, Santa Cruz, CA, USA; cat. no. sc-2357) or anti-mouse IgG (1:5000, Cell Signaling Technology, Danvers, MA, USA, cat. no. 7076S,) at room temperature for 1 h. The membrane was washed three times with TBST for 10 min and protein bands were visualized with enhanced chemiluminescent substrate (Thermo Fisher Scientific, Waltham, MA, USA, cat. no. 34577). Protein levels were quantified with ImageJ software and the ratios of nitrated proteins, BDNF, and PV/β-actin were calculated.

2.10. Fluoro-Jade B (FJB) Staining

The rat brain sections were washed in distilled water for 10 min and then incubated in an 80% alcohol solution containing 1% sodium hydroxide. The sections were transferred to a 70% alcohol for 2 min. Then, the sections were incubated with a 0.06% potassium permanganate solution for 10 min. Next, the sections were rinsed in distilled water for 2 min, incubated in 0.01% FJB (Histo-Chem, Jefferson, AR, USA) with 0.1% acetic acid at room temperature for 15 min, dehydrated, and mounted with DPX and glass coverslips. The brain slide was examined by fluorescence microscopy. For the quantification of FJB+ neurons, two researchers calculated the number of FJB+ neurons in each randomized microscopic field of PFC (200X) independently from each rat by using ImageJ and the results were the average values of numbers of each rat.

2.11. Statistical Analysis

Data analysis was performed using Prism v8.0. Values obtained from behavioral experiments were expressed as mean ± standard error, and other values were all presented as mean ± standard deviation. Y-maze data were analyzed by the Kruskal–Wallis test, and the animal experiments were performed at least three times. p values < 0.05 were considered statistically significant.

3. Results

3.1. BM Alleviates Cognitive Deficits and Increases Cerebral Blood Flow in Rats with BCCAO

The cognition and memory ability of rats were tested with the Y-maze test four weeks after surgery. The rate of spontaneous alternations was lower in the BCCAO group than in the sham group ($p < 0.05$). However, BCCAO+BM rats showed a significantly higher rate of spontaneous alternations than the BCCAO rats ($p < 0.05$), indicating an improvement in short-term memory. There was no significant difference in performance between the BCCAO+BM and sham groups (Figure 1B). The number of maze arm entries did not differ significantly between the three groups ($p > 0.05$; Figure 1C), indicating that there was no impairment of motor function and that BM specifically improved cognitive function and memory in BCCAO rats. SPECT images obtained using the 99mTc-HMPAO tracer revealed that BM increased cerebral blood flow after surgery (Figure 1D,E).

3.2. BM Improves LTP and Increases BDNF Expression

To investigate the effect of BM on the BCCAO-induced inhibition of LTP at the CA3–CA1 synapse, we analyzed the slope of fEPSPs, a marker of short-term synaptic plasticity. Evoked synaptic responses were assessed by calculating the average slope of fEPSPs 5 to 60 min after TBS. High-frequency stimulation-induced robust LTP in the sham and BCCAO+BM groups (Figure 2A,B). The amplitude of fEPSPs increased by 175.45% at 30 min and by 154.65% 60 min after TBS in the sham group; this was significantly greater than the increases observed in the BCCAO group (125.0% and 105.2%, respectively; $F [2, 237] = 5$, $p < 0.0001$; Figure 2C). Meanwhile, BM treatment reversed the BCCAO-induced suppression of LTP ($p = 0.017$; Figure 2C), with fEPSP amplitudes of 163.44% at 30 min and 146.70% at 60 min after TBS. Similar trends were observed in the slope of fEPSPs after TBS, which was significantly lower in the BCCAO group than in the sham group ($p < 0.0001$; Figure 2D) and restored by BM treatment ($p = 0.017$; Figure 2D). These data indicate that BCCAO

inhibited LTP in the hippocampus and that the effect was partially reversed by treatment with BM.

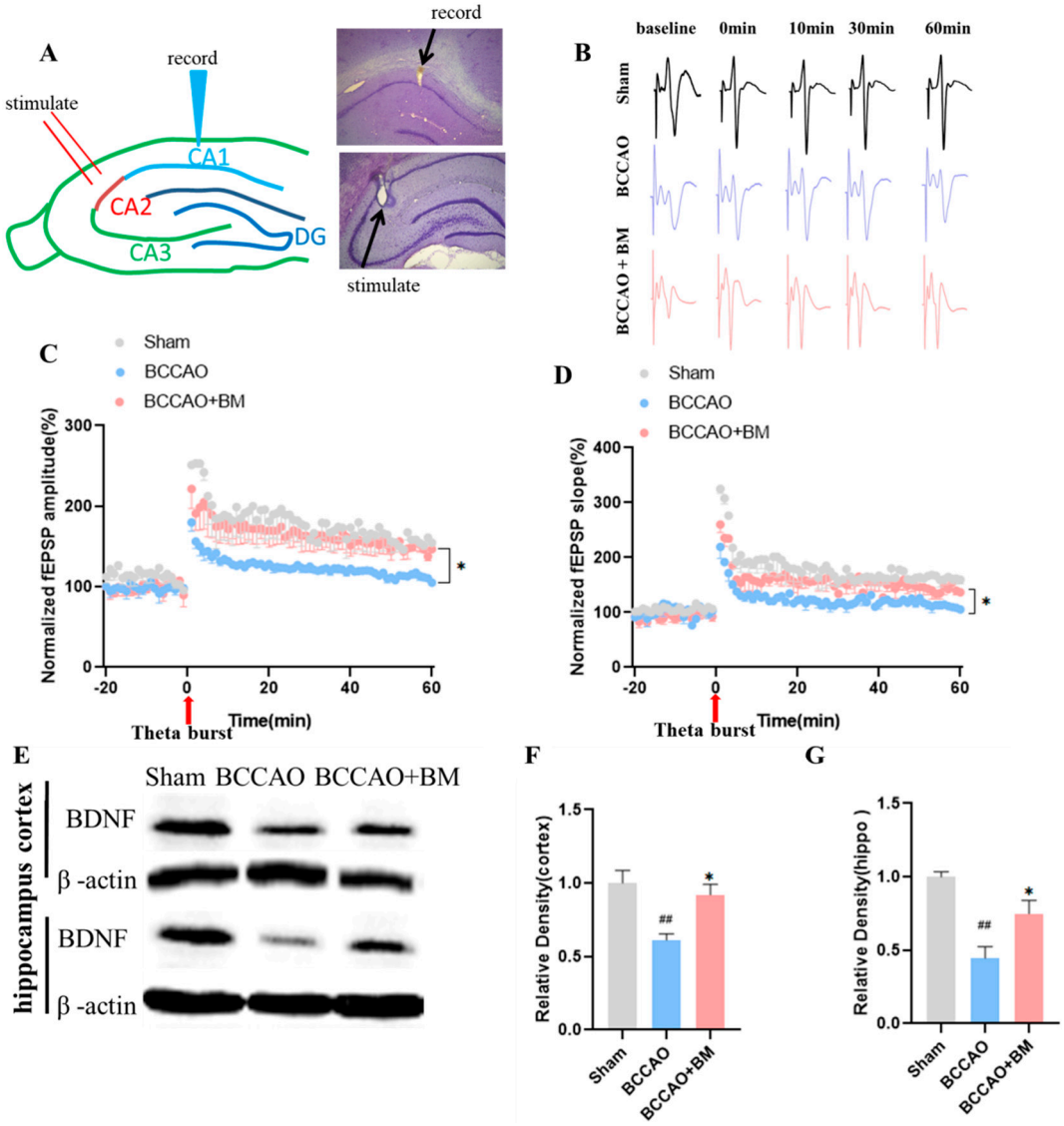

Figure 2. Botanical mixture improves LTP and increases BDNF expression in rats with BCCAO. (**A**) Schematic illustration and location of the stimulation site for LTP and recording site in the hippocampus CA1 area. (**B**) Representative fEPSP traces. (**C**,**D**) Time-dependent changes in amplitude and slope of fEPSP potentiation in the hippocampus CA1 area following LTP induction. (**E**) BDNF and β-actin expression in the PFC and hippocampus. (**F**,**G**) Quantification of BDNF protein levels in the PFC (**F**) and hippocampus (**G**). Values are mean ± SEM of normalized amplitudes or slope of fEPSPs (one-way analysis of variance: amplitude, F [2, 237] = 5, $p < 0.0001$; slope: F [2, 237] = 3, $p < 0.0001$). ## $p < 0.01$ vs. sham; * $p < 0.05$, vs. BCCAO ($n = 6$ per group [LTP] and 4 [BDNF]).

BDNF is involved in neuroplasticity and may directly regulate the structure and number of synapses [21]. BDNF protein levels were significantly lower in the prefrontal cortex (PFC) ($p = 0.0034$; Figure 2E,F) and hippocampus ($p = 0.0011$; Figure 2E,G) of BCCAO rats than in sham rats, as determined by Western blotting. However, BM reversed this decrease to some extent ($p < 0.05$; Figure 2E–G).

3.3. BM Alleviates Damage to PV+ Neurons and Neuron Death in the Cortex and Hippocampus of BCCAO Rats

The neuroprotective effect of BM in the PFC and hippocampus was examined by FJB staining and immunohistochemistry. There were more FJB+ neurons in the PFC of the BCCAO rats than in the sham group (Figure 3A), indicating that BCCAO increased neuron death. In contrast, there were fewer FJB+ neurons in BCCAO+BM rats than in BCCAO rats.

The Ca^{2+}-binding protein PV is highly expressed in gamma-aminobutyric acid (GABA) ergic interneurons [22] and modulates cognitive function. The sham group had many PV+ neurons in the PFC and hippocampus, and these had an orderly arrangement with clear nuclei (Figure 3A). However, the number of PV+ neurons and dendritic spines in the PFC and hippocampus was significantly lower in the BCCAO group ($p < 0.01$; Figure 3B–D). BM treatment restored the number of PV+ neurons relative to the BCCAO group. The results obtained by immunohistochemistry were confirmed by Western blotting; PV protein levels were lower in the PFC ($p < 0.001$) and hippocampus ($p < 0.01$) of BCCAO rats than those in sham rats, but this effect was abrogated ($p < 0.05$) in BCCAO+BM rats (Figure 3E–G). These data indicate that BM reduced damage to PV+ neurons and increased PV expression, suggesting a protective effect on GABAergic interneurons. Immunohistochemical detection of NeuN revealed that there was no significant differences in the expression of NeuN+ neurons in the PFC and hippocampus across groups ($p > 0.05$; Figure 3H–J).

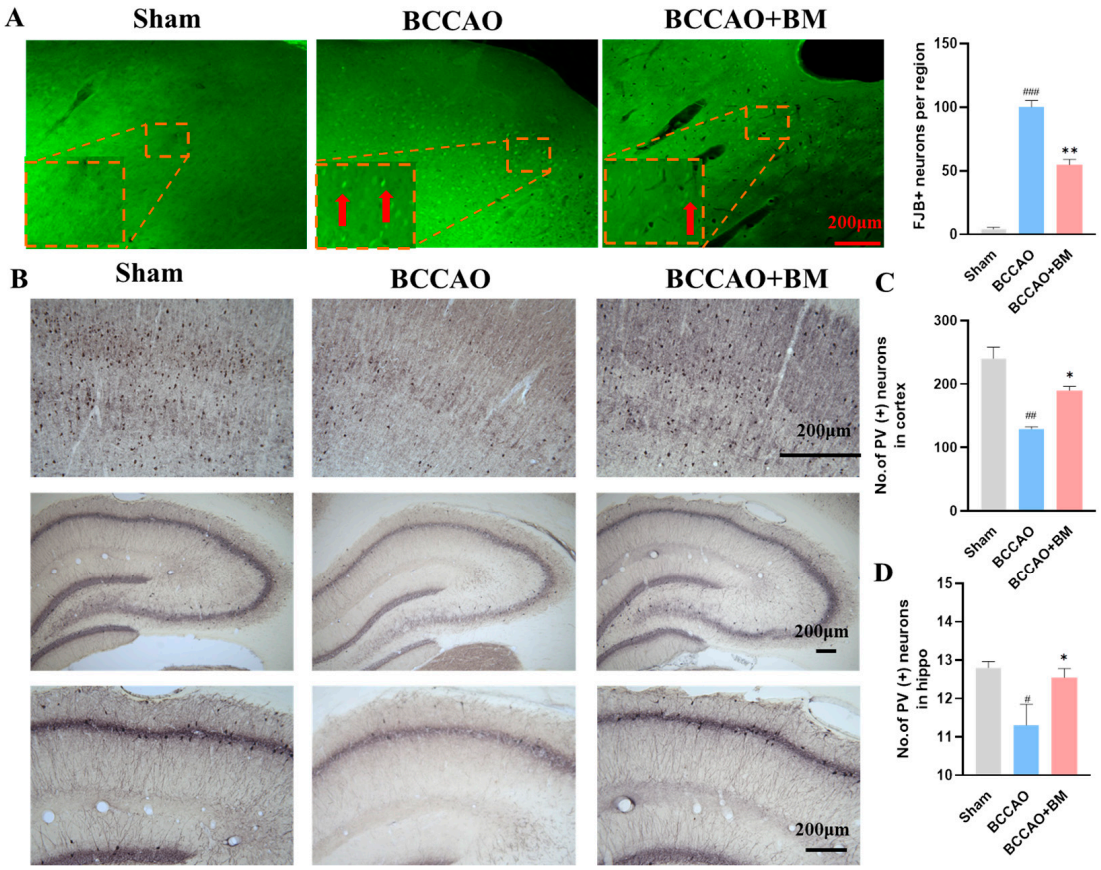

Figure 3. *Cont.*

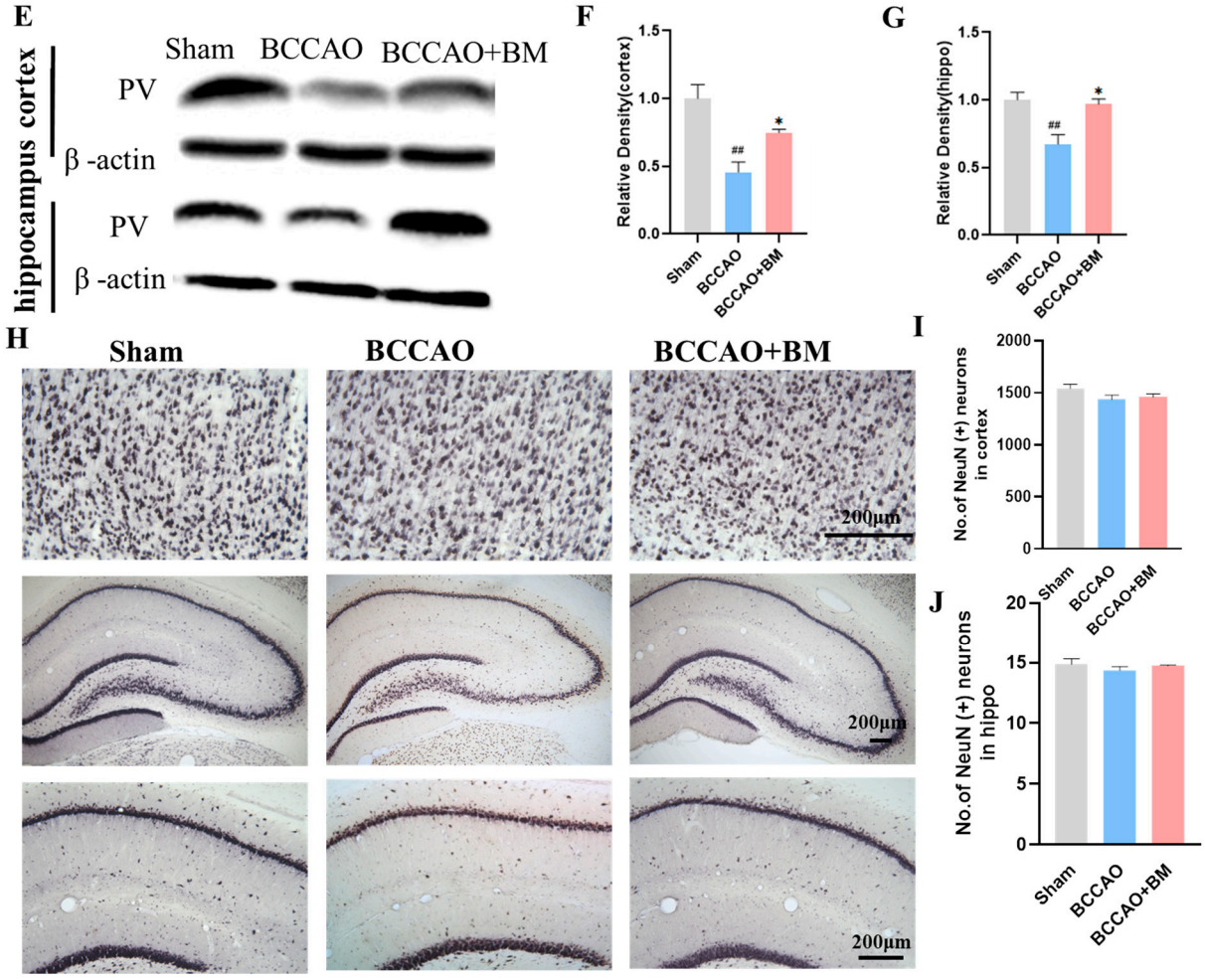

Figure 3. Botanical mixture administration alleviates neuronal damage and death in the PFC and hippocampus of rats with BCCAO. (**A**) FJB staining in the PFC (FJB+ neurons were showed with red arrow) and the quantification of FJB+ neurons in each group. Scale bar, 200 μm. (**B**) PV immunolabeling in the PFC and hippocampus. (**C**,**D**) Quantitative analysis of the PV-positive neurons in the PFC (**C**) and the whole hippocampus (**D**). Scale bar, 200 μm. (**E**) PV and β-actin expression in the PFC and hippocampus. (**F**,**G**) Quantification of PV protein levels in the PFC (**F**) and hippocampus (**G**). (**H**) NeuN immunolabeling in the PFC and hippocampus. Scale bar, 200 μm. (**I**,**J**) Quantification of NeuN protein levels in the PFC and the whole hippocampus. # $p < 0.05$, ## $p < 0.01$, ### $p < 0.001$ vs. sham; * $p < 0.05$, ** $p < 0.01$ vs. BCCAO ($n = 4$ per group).

3.4. BM Reduces Oxidative Stress and GFAP Expression

VD is associated with a reduction in antioxidant function and an increase in the production of ROS-related oxidative markers [23,24]. As nitrotyrosine is a marker of oxidative stress [25], we quantified its expression immunohistochemically. The number of neurons with nitrotyrosine immunoreactivity in the PFC and hippocampus was significantly higher in the BCCAO group than in the sham group ($p < 0.01$; Figure 4A,C) but was reduced by BM treatment ($p = 0.0106$ for the PFC and $p = 0.0364$ for the hippocampus). These results indicate that BM protects neurons by reducing injury caused by oxidative stress.

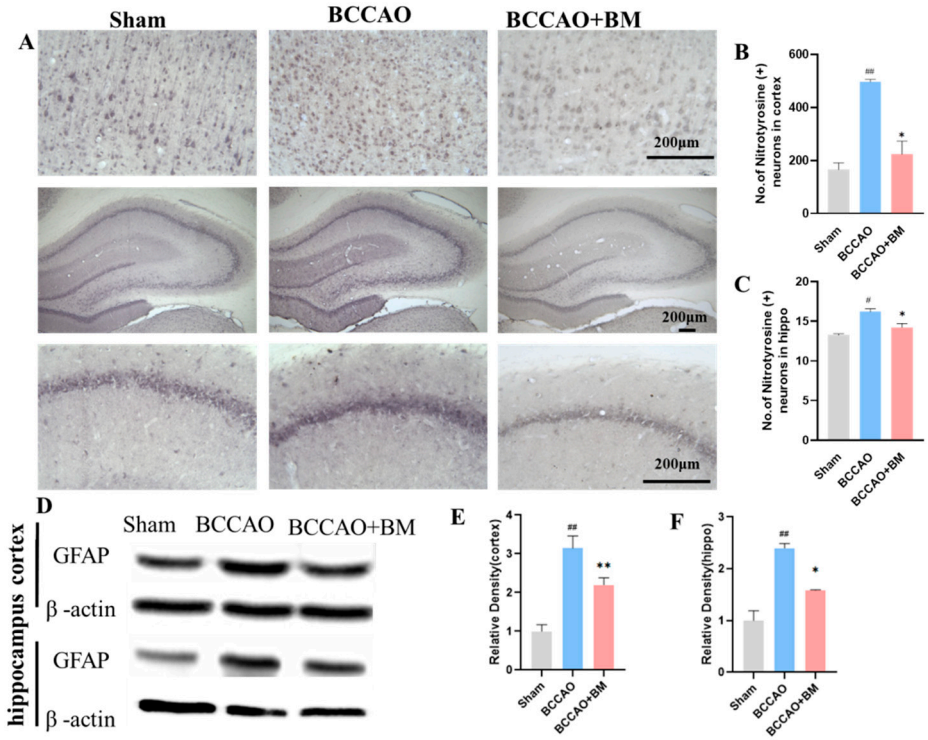

Figure 4. Botanical mixture alleviates oxidative stress and reduces GFAP expression. (**A**) Nitrotyrosine immunolabeling in the PFC and hippocampus. Scale bar, 200 μm. (**B**,**C**) Quantification of nitrotyrosine levels (strength of nitrotyrosine positive cells) in the PFC and hippocampus. (**D**) GFAP and β-actin expression in the PFC and hippocampus. (**E**,**F**) Quantification of the GFAP levels in the PFC (**E**) and hippocampus (**F**). # $p < 0.05$, ## $p < 0.01$ vs. sham; * $p < 0.05$, ** $p < 0.01$ vs. BCCAO ($n = 4$ per group).

GFAP is a marker of activated astrocytes that are upregulated in VD [26]. Accordingly, GFAP expression was significantly higher in the PFC (F [2, 9] = 84.25, $p < 0.001$; Figure 4D,E) and hippocampus (F [2, 9] = 33.02, $p < 0.001$; Figure 4F) of BCCAO rats than in sham rats, but BM lowered this increase ($p < 0.01$).

4. Discussion

The results of the present study demonstrate that the BM composed of garlic containing NO metabolite, fermented *S. baicalensis*, and *R. rosea* reduced neuron damage and death, increased cerebral blood flow, enhanced BDNF expression, reduced GFAP expression, and alleviated cognitive deficits in a rat model of VD. Moreover, BM reduced the loss of PV GABAergic interneurons caused by BCCAO and enhanced LTP, which may underlie the improvement in cognitive performance observed with BM treatment.

BCCAO in rats has been widely used to investigate chronic cerebral hypoperfusion associated with VD. Blood flow in the cortex of BCCAO rats is reduced by 42–50% in the three days post-surgery and remains at just 66% of the normal blood flow rate after four or more weeks [27,28]. Another study indicated that the blood flow in the hippocampal CA1 area was reduced from 78.4% on day 3 to 66% on week 4 [27]. Thus, the CA1 area of the hippocampus is more sensitive to ischemia than the cerebral cortex [29]. Using SPECT imaging, we found that BM increased blood flow in the brain of BCCAO rats; it also restored spatial working memory.

NO is an important multifunctional messenger molecule in the brain that plays a key role in learning and memory. NO has neuroprotective and cognition-enhancing effects and has therapeutic potential for the treatment of neurodegenerative diseases [30,31]. Fermented garlic extract contains NO metabolites such as nitrite and is considered an important medicinal plant owing to its immunomodulatory, antioxidant, antimicrobial, antidiabetic, anti-inflammatory, and antihypertensive activities [32–34]. Garlic also contains

polyphenols and organosulfur compounds that destroy free radicals and suppress ROS generation to protect against neuronal injury [35,36]. *S. baicalensis* has anti-inflammatory, antidiabetic, antibacterial, anti-allergic, antiviral, and antihypertensive effects, and has been widely used in Oriental medicine for the treatment of brain diseases [37,38]. Baicalein, baicalin, oroxylin, and wogonin are pharmacologically active substances in *S. baicalensis* that have a strong antioxidant activity and inhibit oxidative stress caused by ROS, thereby suppressing inflammation and preventing ischemic cell damage [39]. *S. baicalensis* was shown to protect neurons from oxidative stress and reduce brain damage in ischemic brain injury models [40]; it also promotes the expression of BDNF, which is involved in neuroplasticity [41,42]. *R. rosea* has been used to alleviate anxiety and prevent high-altitude sickness and was reported to improve learning and memory and increase neurotransmitter levels, with demonstrated antioxidant activity [14,43,44]. Many of the above effects were observed in the present study in BCCAO rats treated with the combination of the three substances.

VD is characterized by an increase in ROS production, neuronal damage, activation of microglia and astrogliosis, memory deficits, and behavioral and mood changes [45–47]. Hippocampal LTP has been used as an electrophysiologic indicator of the formation and maintenance of memory at the synaptic level [48]. LTP was decreased to 40–77% of the baseline level in the CA1 area of the hippocampus of BCCAO rats compared with sham-operated rats four weeks after surgery [49,50]. Additionally, 8 and 16 weeks after BCCAO, the degree of LTP reduction in the CA1 region was similar to that observed in the early stage after BCCAO [50]. We found a similar degree of LTP reduction in the CA1 area four weeks post-surgery; additionally, LTP was greater in the BCCAO+BM group than in the BCCAO group. This is likely related to the observed increase in BDNF—which plays a critical role in hippocampal CA1-related memory and LTP development [51–53]—induced by BM treatment in the present study.

Intracellular ATP concentration is closely related to neuron death and rapidly decreases from the first three days and up to eight weeks after BCCAO [18,46,47]. Thus, damage to neurons begins in the early stages of BCCAO due to a decrease in blood flow and ATP concentration. In our study, the loss of neurons in BCCAO rats was demonstrated by FJB staining, but there were fewer FJB+ neurons in the BCCAO+BM group than in the BCCAO group. As BCCAO did not alter the number of NeuN+ neurons, we concluded that most of the FJB+ neurons were PV+ GABAergic interneurons. PV is a Ca^{2+}-binding protein known to protect neurons from Ca^{2+}-mediated cell death by accelerating Ca^{2+} removal after neuronal injury [54]. AD patients have reduced PV+ interneuron counts, which was related to memory decline [55,56]. BDNF selectively regulates PV expression and stimulates dendrite growth in a subset of GABAergic interneurons by activating the phospholipase C gamma pathway [57]. We found that the expression levels of PV and BDNF were significantly decreased in BCCAO rats, but this was reversed by BM treatment. Our results suggest that PV+ neurons are highly sensitive to BCCAO.

Besides neuron loss and decreased synaptic plasticity, the activation of microglia and astrocytes is related to memory and cognitive deficits in VD. Oxidative stress is a major feature of VD [38], and inflammatory cytokines have been linked to neuronal dysfunction and cognitive decline [58]. Nitrotyrosine is a marker for oxidative stress, cell damage, and inflammation that induces the activation of microglia and astrocytes [25]. In this study, nitrotyrosine levels were significantly increased in the BCCAO group but were reduced by BM treatment.

A limitation of our study is that the molecular mechanism and signaling pathways underlying the effects of BM were not investigated. In the future, a BCCAO rat model in which the synthesis of endogenous NO can be inhibited by the NOS inhibitor-l-NAME can be established to explore this question.

5. Conclusions

NO metabolites in BM composed of fermented garlic extract, fermented *S. baicalensis*, and *R. rosea* alleviated cerebral hypoperfusion injury in a BCCAO rat model. This was

accompanied by enhanced LTP induction, increased cerebral blood flow, the upregulation of the neuroplasticity-related factor BDNF as well as PV, and decreased GFAP expression and neuron death in the hippocampus, with a corresponding improvement in spatial memory. These results suggest that BM can directly enhance neuroplasticity in the brain by improving blood flow and exerting an antioxidant effect, highlighting its therapeutic potential for the treatment of VD.

Author Contributions: The initial idea for this manuscript was from M.-S.K.; X.Z. and S.-B.Y. wrote and revised the manuscript; L.C. and K.H. edited the manuscript; M.-S.K. and S.-B.Y. read, reviewed, and approved the final manuscript. All authors have read and agreed to the published version of the manuscript.

Funding: This study was funded by the Science and Technology Project Founded by the Education Department of Jiangxi Province (GJJ211813, GJJ211812), the Provincial Natural Science Foundation of Jiangxi Province (20224BAB206040), Research project of Cognitive Science and Transdisciplinary Studies Center of Jiangxi Province (RZYB202201) and the Administration of Traditional Chinese Medicine of Jiangxi Province (2022B1010).

Institutional Review Board Statement: The study was conducted in accordance with the Declaration of Helsinki, and approved by the Laboratory Animal Ethics Committee of Wonkwang University.

Informed Consent Statement: Not applicable.

Data Availability Statement: Not applicable.

Acknowledgments: We sincerely thank for HumanEnos (South Korea) for supply of Nitric Oxide Metabolite.

Conflicts of Interest: The authors declare no conflict of interest.

References

1. O'Brien, J.T.; Thomas, A. Vascular dementia. *Lancet* **2015**, *386*, 1698–1706. [CrossRef] [PubMed]
2. Sun, M.K. Potential Therapeutics for Vascular Cognitive Impairment and Dementia. *Curr. Neuropharmacol.* **2018**, *16*, 1036–1044. [CrossRef] [PubMed]
3. Forstermann, U.; Sessa, W.C. Nitric oxide synthases: Regulation and function. *Eur. Heart J.* **2012**, *33*, 829–837. [CrossRef]
4. Picon-Pages, P.; Garcia-Buendia, J.; Munoz, F.J. Functions and dysfunctions of nitric oxide in brain. *Biochim. Biophys. Acta Mol. Basis Dis.* **2019**, *1865*, 1949–1967. [CrossRef] [PubMed]
5. Zhu, H.Y.; Hong, F.F.; Yang, S.L. The Roles of Nitric Oxide Synthase/Nitric Oxide Pathway in the Pathology of Vascular Dementia and Related Therapeutic Approaches. *Int. J. Mol. Sci.* **2021**, *22*, 4540. [CrossRef] [PubMed]
6. Amdahl, M.B.; DeMartino, A.W.; Gladwin, M.T. Inorganic nitrite bioactivation and role in physiological signaling and therapeutics. *Biol. Chem.* **2019**, *401*, 201–211. [CrossRef]
7. Piknova, B.; Park, J.W.; Thomas, S.M.; Tunau-Spencer, K.J.; Schechter, A.N. Nitrate and Nitrite Metabolism in Aging Rats: A Comparative Study. *Nutrients* **2023**, *15*, 2490. [CrossRef] [PubMed]
8. Gokalp, F. The inhibition effect of garlic-derived compounds on human immunodeficiency virus type 1 and saquinavir. *J. Biochem. Mol. Toxicol.* **2018**, *32*, e22215. [CrossRef]
9. Lee, Y.J.; Lee, D.; Shin, S.M.; Lee, J.S.; Chun, H.S.; Quan, F.-S.; Shin, J.H.; Lee, G.-J. Potential protective effects of fermented garlic extract on myocardial ischemia-reperfusion injury utilizing in vitro and ex vivo models. *J. Funct. Foods* **2017**, *33*, 278–285. [CrossRef]
10. Park, B.M.; Cha, S.A.; Kim, H.Y.; Kang, D.K.; Yuan, K.; Chun, H.; Chae, S.W.; Kim, S.H. Fermented garlic extract decreases blood pressure through nitrite and sGC-cGMP-PKG pathway in spontaneously hypertensive rats. *J. Funct. Foods* **2016**, *22*, 156–165. [CrossRef]
11. Baik, J.S.; Min, J.H.; Ju, S.M.; Ahn, J.H.; Ko, S.H.; Chon, H.S.; Kim, M.S.; Shin, Y.I. Effects of Fermented Garlic Extract Containing Nitric Oxide Metabolites on Blood Flow in Healthy Participants: A Randomized Controlled Trial. *Nutrients* **2022**, *14*, 5238. [CrossRef]
12. Choi, J.H.; Choi, A.Y.; Yoon, H.; Choe, W.; Yoon, K.S.; Ha, J.; Yeo, E.J.; Kang, I. Baicalein protects HT22 murine hippocampal neuronal cells against endoplasmic reticulum stress-induced apoptosis through inhibition of reactive oxygen species production and CHOP induction. *Exp. Mol. Med.* **2010**, *42*, 811–822. [CrossRef] [PubMed]
13. Lei, K.; Shen, Y.; He, Y.; Zhang, L.; Zhang, J.; Tong, W.; Xu, Y.; Jin, L. Baicalin Represses C/EBPbeta via Its Antioxidative Effect in Parkinson's Disease. *Oxidative Med. Cell. Longev.* **2020**, *2020*, 8951907. [CrossRef] [PubMed]
14. Ma, G.P.; Zheng, Q.; Xu, M.B.; Zhou, X.L.; Lu, L.; Li, Z.X.; Zheng, G.Q. *Rhodiola rosea* L. Improves Learning and Memory Function: Preclinical Evidence and Possible Mechanisms. *Front. Pharmacol.* **2018**, *9*, 1415. [CrossRef] [PubMed]

15. Abidov, M.; Crendal, F.; Grachev, S.; Seifulla, R.; Ziegenfuss, T. Effect of extracts from *Rhodiola rosea* and *Rhodiola crenulata* (*Crassulaceae*) roots on ATP content in mitochondria of skeletal muscles. *Bull. Exp. Biol. Med.* **2003**, *136*, 585–587. [CrossRef] [PubMed]
16. Panossian, A.; Wikman, G.; Sarris, J. Rosenroot (*Rhodiola rosea*): Traditional use, chemical composition, pharmacology and clinical efficacy. *Phytomedicine* **2010**, *17*, 481–493. [CrossRef] [PubMed]
17. Zhang, J.J.; Li, X.Q.; Sun, J.W.; Jin, S.H. Nitric oxide functions as a signal in ultraviolet-B-induced baicalin accumulation in *Scutellaria baicalensis* suspension cultures. *Int. J. Mol. Sci.* **2014**, *15*, 4733–4746. [CrossRef] [PubMed]
18. Farkas, E.; Luiten, P.G.; Bari, F. Permanent, bilateral common carotid artery occlusion in the rat: A model for chronic cerebral hypoperfusion-related neurodegenerative diseases. *Brain Res. Rev.* **2007**, *54*, 162–180. [CrossRef]
19. Washida, K.; Hattori, Y.; Ihara, M. Animal Models of Chronic Cerebral Hypoperfusion: From Mouse to Primate. *Int. J. Mol. Sci.* **2019**, *20*, 6176. [CrossRef]
20. Polopalli, S.; Yetukuri, A.R.; Danduga, R.; Kola, P.K. A prognostic study on the effect of post-traumatic stress disorder on cerebral ischaemia reperfusion-induced stroke. *World J. Biol. Psychiatry* **2022**, *23*, 136–150. [CrossRef] [PubMed]
21. Gallo, E.F.; Iadecola, C. Neuronal nitric oxide contributes to neuroplasticity-associated protein expression through cGMP, protein kinase G, and extracellular signal-regulated kinase. *J. Neurosci.* **2011**, *31*, 6947–6955. [CrossRef] [PubMed]
22. Long, Q.; Upadhya, D.; Hattiangady, B.; Kim, D.K.; An, S.Y.; Shuai, B.; Prockop, D.J.; Shetty, A.K. Intranasal MSC-derived A1-exosomes ease inflammation, and prevent abnormal neurogenesis and memory dysfunction after status epilepticus. *Proc. Natl. Acad. Sci. USA* **2017**, *114*, E3536–E3545. [CrossRef] [PubMed]
23. Wilson, E.N.; Do Carmo, S.; Iulita, M.F.; Hall, H.; Austin, G.L.; Jia, D.T.; Malcolm, J.C.; Foret, M.K.; Marks, A.R.; Butterfield, D.A.; et al. Microdose Lithium NP03 Diminishes Pre-Plaque Oxidative Damage and Neuroinflammation in a Rat Model of Alzheimer's-like Amyloidosis. *Curr. Alzheimer Res.* **2018**, *15*, 1220–1230. [CrossRef] [PubMed]
24. Do Carmo, S.; Crynen, G.; Paradis, T.; Reed, J.; Iulita, M.F.; Ducatenzeiler, A.; Crawford, F.; Cuello, A.C. Hippocampal Proteomic Analysis Reveals Distinct Pathway Deregulation Profiles at Early and Late Stages in a Rat Model of Alzheimer's-like Amyloid Pathology. *Mol. Neurobiol.* **2018**, *55*, 3451–3476. [CrossRef]
25. Butterfield, D.A.; Reed, T.; Sultana, R. Roles of 3-nitrotyrosine- and 4-hydroxynonenal-modified brain proteins in the progression and pathogenesis of Alzheimer's disease. *Free Radic. Res.* **2011**, *45*, 59–72. [CrossRef] [PubMed]
26. Liu, Q.; Bhuiyan, M.I.H.; Liu, R.; Song, S.; Begum, G.; Young, C.B.; Foley, L.M.; Chen, F.; Hitchens, T.K.; Cao, G.; et al. Attenuating vascular stenosis-induced astrogliosis preserves white matter integrity and cognitive function. *J. Neuroinflamm.* **2021**, *18*, 187. [CrossRef]
27. Otori, T.; Katsumata, T.; Muramatsu, H.; Kashiwagi, F.; Katayama, Y.; Terashi, A. Long-term measurement of cerebral blood flow and metabolism in a rat chronic hypoperfusion model. *Clin. Exp. Pharmacol. Physiol.* **2003**, *30*, 266–272. [CrossRef] [PubMed]
28. Mansour, A.; Niizuma, K.; Rashad, S.; Sumiyoshi, A.; Ryoke, R.; Endo, H.; Endo, T.; Sato, K.; Kawashima, R.; Tominaga, T. A refined model of chronic cerebral hypoperfusion resulting in cognitive impairment and a low mortality rate in rats. *J. Neurosurg.* **2018**, *131*, 892–902. [CrossRef]
29. Nikonenko, A.G.; Radenovic, L.; Andjus, P.R.; Skibo, G.G. Structural features of ischemic damage in the hippocampus. *Anat. Rec.* **2009**, *292*, 1914–1921. [CrossRef]
30. Thatcher, G.R.; Bennett, B.M.; Reynolds, J.N. Nitric oxide mimetic molecules as therapeutic agents in Alzheimer's disease. *Curr. Alzheimer Res.* **2005**, *2*, 171–182. [CrossRef] [PubMed]
31. Dubey, H.; Gulati, K.; Ray, A. Amelioration by nitric oxide (NO) mimetics on neurobehavioral and biochemical changes in experimental model of Alzheimer's disease in rats. *Neurotoxicology* **2018**, *66*, 58–65. [CrossRef]
32. Ashraf, R.; Khan, R.A.; Ashraf, I.; Qureshi, A.A. Effects of *Allium sativum* (garlic) on systolic and diastolic blood pressure in patients with essential hypertension. *Pak. J. Pharm. Sci.* **2013**, *26*, 859–863.
33. Morales-Gonzalez, J.A.; Madrigal-Bujaidar, E.; Sanchez-Gutierrez, M.; Izquierdo-Vega, J.A.; Valadez-Vega, M.D.C.; Alvarez-Gonzalez, I.; Morales-Gonzalez, A.; Madrigal-Santillan, E. Garlic (*Allium sativum* L.): A Brief Review of Its Antigenotoxic Effects. *Foods* **2019**, *8*, 343. [CrossRef]
34. Naderi, R.; Mohaddes, G.; Mohammadi, M.; Alihemmati, A.; Badalzadeh, R.; Ghaznavi, R.; Ghyasi, R.; Mohammadi, S. Preventive effects of garlic (*Allium sativum*) on oxidative stress and histopathology of cardiac tissue in streptozotocin-induced diabetic rats. *Acta Physiol. Hung.* **2015**, *102*, 380–390. [CrossRef] [PubMed]
35. Colin-Gonzalez, A.L.; Santana, R.A.; Silva-Islas, C.A.; Chanez-Cardenas, M.E.; Santamaria, A.; Maldonado, P.D. The antioxidant mechanisms underlying the aged garlic extract- and S-allylcysteine-induced protection. *Oxidative Med. Cell. Longev.* **2012**, *2012*, 907162. [CrossRef]
36. Farooqui, T.; Farooqui, A.A. Neuroprotective Effects of Garlic in Model Systems of Neurodegenerative Diseases. In *Role of the Mediterranean Diet in the Brain and Neurodegenerative Diseases*; Academic Press: Cambridge, MA, USA, 2018; pp. 253–269.
37. Zhao, T.; Tang, H.; Xie, L.; Zheng, Y.; Ma, Z.; Sun, Q.; Li, X. *Scutellaria baicalensis* Georgi. (Lamiaceae): A review of its traditional uses, botany, phytochemistry, pharmacology and toxicology. *J. Pharm. Pharmacol.* **2019**, *71*, 1353–1369. [CrossRef]
38. Tu, T.H.; Liou, D.Y.; Lin, D.Y.; Yang, H.C.; Chen, C.J.; Huang, M.C.; Huang, W.C.; Tsai, M.J.; Cheng, H. Characterizing the Neuroprotective Effects of S/B Remedy (*Scutellaria baicalensis* Georgi and *Bupleurum scorzonerifolfium* Willd) in Spinal Cord Injury. *Molecules* **2019**, *24*, 1885. [CrossRef]

39. Wang, Z.L.; Wang, S.; Kuang, Y.; Hu, Z.M.; Qiao, X.; Ye, M. A comprehensive review on phytochemistry, pharmacology, and flavonoid biosynthesis of *Scutellaria baicalensis*. *Pharm. Biol.* **2018**, *56*, 465–484. [CrossRef]
40. Gaire, B.P.; Moon, S.K.; Kim, H. *Scutellaria baicalensis* in stroke management: Nature's blessing in traditional Eastern medicine. *Chin. J. Integr. Med.* **2014**, *20*, 712–720. [CrossRef]
41. Kim, D.H.; Lee, Y.; Lee, H.E.; Park, S.J.; Jeon, S.J.; Jeon, S.J.; Cheong, J.H.; Shin, C.Y.; Son, K.H.; Ryu, J.H. Oroxylin A enhances memory consolidation through the brain-derived neurotrophic factor in mice. *Brain Res. Bull.* **2014**, *108*, 67–73. [CrossRef] [PubMed]
42. Fong, S.Y.; Wong, Y.C.; Zuo, Z. Development of a SPE-LC/MS/MS method for simultaneous quantification of baicalein, wogonin, oroxylin A and their glucuronides baicalin, wogonoside and oroxyloside in rats and its application to brain uptake and plasma pharmacokinetic studies. *J. Pharm. Biomed. Anal.* **2014**, *97*, 9–23. [CrossRef]
43. Spasov, A.A.; Wikman, G.K.; Mandrikov, V.B.; Mironova, I.A.; Neumoin, V.V. A double-blind, placebo-controlled pilot study of the stimulating and adaptogenic effect of *Rhodiola rosea* SHR-5 extract on the fatigue of students caused by stress during an examination period with a repeated low-dose regimen. *Phytomedicine* **2000**, *7*, 85–89. [CrossRef] [PubMed]
44. Zhang, L.; Yu, H.; Sun, Y.; Lin, X.; Chen, B.; Tan, C.; Cao, G.; Wang, Z. Protective effects of salidroside on hydrogen peroxide-induced apoptosis in SH-SY5Y human neuroblastoma cells. *Eur. J. Pharmacol.* **2007**, *564*, 18–25. [CrossRef] [PubMed]
45. Saxena, A.K.; Abdul-Majeed, S.S.; Gurtu, S.; Mohamed, W.M. Investigation of redox status in chronic cerebral hypoperfusion-induced neurodegeneration in rats. *Appl. Transl. Genom.* **2015**, *5*, 30–32. [CrossRef] [PubMed]
46. Cechetti, F.; Pagnussat, A.S.; Worm, P.V.; Elsner, V.R.; Ben, J.; da Costa, M.S.; Mestriner, R.; Weis, S.N.; Netto, C.A. Chronic brain hypoperfusion causes early glial activation and neuronal death, and subsequent long-term memory impairment. *Brain Res. Bull.* **2012**, *87*, 109–116. [CrossRef] [PubMed]
47. Jing, Z.; Shi, C.; Zhu, L.; Xiang, Y.; Chen, P.; Xiong, Z.; Li, W.; Ruan, Y.; Huang, L. Chronic cerebral hypoperfusion induces vascular plasticity and hemodynamics but also neuronal degeneration and cognitive impairment. *J. Cereb. Blood Flow. Metab.* **2015**, *35*, 1249–1259. [CrossRef] [PubMed]
48. Tamano, H.; Takiguchi, M.; Shimaya, R.; Adlard, P.A.; Bush, A.I.; Takeda, A. Extracellular Zn(2+)-independently attenuated LTP by human amyloid beta1-40 and rat amyloid beta1-42. *Biochem. Biophys. Res. Commun.* **2019**, *514*, 888–892. [CrossRef]
49. He, Z.; Huang, L.; Wu, Y.; Wang, J.; Wang, H.; Guo, L. DDPH: Improving cognitive deficits beyond its alpha 1-adrenoceptor antagonism in chronic cerebral hypoperfused rats. *Eur. J. Pharmacol.* **2008**, *588*, 178–188. [CrossRef] [PubMed]
50. Luo, P.; Lu, Y.; Li, C.; Zhou, M.; Chen, C.; Lu, Q.; Xu, X.; He, Z.; Guo, L. Long-lasting spatial learning and memory impairments caused by chronic cerebral hypoperfusion associate with a dynamic change of HCN1/HCN2 expression in hippocampal CA1 region. *Neurobiol. Learn. Mem.* **2015**, *123*, 72–83. [CrossRef] [PubMed]
51. Leal, G.; Afonso, P.M.; Salazar, I.L.; Duarte, C.B. Regulation of hippocampal synaptic plasticity by BDNF. *Brain Res.* **2015**, *1621*, 82–101. [CrossRef] [PubMed]
52. De Vincenti, A.P.; Rios, A.S.; Paratcha, G.; Ledda, F. Mechanisms That Modulate and Diversify BDNF Functions: Implications for Hippocampal Synaptic Plasticity. *Front. Cell Neurosci.* **2019**, *13*, 135. [CrossRef] [PubMed]
53. Mokhtari-Zaer, A.; Saadat, S.; Marefati, N.; Hosseini, M.; Boskabady, M.H. Treadmill exercise restores memory and hippocampal synaptic plasticity impairments in ovalbumin-sensitized juvenile rats: Involvement of brain-derived neurotrophic factor (BDNF). *Neurochem. Int.* **2020**, *135*, 104691. [CrossRef] [PubMed]
54. Van Den Bosch, L.; Schwaller, B.; Vleminckx, V.; Meijers, B.; Stork, S.; Ruehlicke, T.; Van Houtte, E.; Klaassen, H.; Celio, M.R.; Missiaen, L.; et al. Protective effect of parvalbumin on excitotoxic motor neuron death. *Exp. Neurol.* **2002**, *174*, 150–161. [CrossRef] [PubMed]
55. Xia, F.; Richards, B.A.; Tran, M.M.; Josselyn, S.A.; Takehara-Nishiuchi, K.; Frankland, P.W. Parvalbumin-positive interneurons mediate neocortical-hippocampal interactions that are necessary for memory consolidation. *eLife* **2017**, *6*, e27868. [CrossRef] [PubMed]
56. Sanchez-Mejias, E.; Nunez-Diaz, C.; Sanchez-Varo, R.; Gomez-Arboledas, A.; Garcia-Leon, J.A.; Fernandez-Valenzuela, J.J.; Mejias-Ortega, M.; Trujillo-Estrada, L.; Baglietto-Vargas, D.; Moreno-Gonzalez, I.; et al. Distinct disease-sensitive GABAergic neurons in the perirhinal cortex of Alzheimer's mice and patients. *Brain Pathol.* **2020**, *30*, 345–363. [CrossRef]
57. Berghuis, P.; Agerman, K.; Dobszay, M.B.; Minichiello, L.; Harkany, T.; Ernfors, P. Brain-derived neurotrophic factor selectively regulates dendritogenesis of parvalbumin-containing interneurons in the main olfactory bulb through the PLCgamma pathway. *J. Neurobiol.* **2006**, *66*, 1437–1451. [CrossRef] [PubMed]
58. Albert, M.S.; DeKosky, S.T.; Dickson, D.; Dubois, B.; Feldman, H.H.; Fox, N.C.; Gamst, A.; Holtzman, D.M.; Jagust, W.J.; Petersen, R.C.; et al. The diagnosis of mild cognitive impairment due to Alzheimer's disease: Recommendations from the National Institute on Aging-Alzheimer's Association workgroups on diagnostic guidelines for Alzheimer's disease. *Alzheimers Dement.* **2011**, *7*, 270–279. [CrossRef]

Disclaimer/Publisher's Note: The statements, opinions and data contained in all publications are solely those of the individual author(s) and contributor(s) and not of MDPI and/or the editor(s). MDPI and/or the editor(s) disclaim responsibility for any injury to people or property resulting from any ideas, methods, instructions or products referred to in the content.